

---



---

**Technical Paper**


---



---

Transactions of the Society of  
Naval Architects of Korea  
Vol. 29, No.3, August 1992  
大韓造船學會論文集  
第 29 卷 第 3 號 1992 年 8 月

## Detection of Sub-Breaking Waves around a Blunt Bow

by

Myung-Soo Shin\*, Young-Gill Lee\*, Eun-Chan Kim\* and Seung-Il Yang\*

### 비대선수 주위의 Sub-Breaking Wave 탐지기법

신명수\*, 이영길\*, 김은찬\*, 양승일\*

#### Abstract

Waves around a practical hull form and a series 60 model are computed by rectangular variable spacing and staggered mesh systems based on MAC(Marker and Cell) method. As a governing equation, the Euler equation is adopted. The comparison indicates that the computed waves are in good agreement with the measured results and that the MAC method is useful. On the other hand, a critical condition for the appearance of sub-breaking waves derived from the inviscid instability analysis is applied to the calculated flow field around a blunt bow. It is confirmed that the derived condition detects well the appearance of sub-breaking waves.

#### 요 약

시리즈 60과 실제 선형주위의 파도를 MAC(Marker And Cell) 법에 의해 격자간격이 변화하는 Staggered좌표계에서 계산하였다. 지배방정식으로는 오일러(Euler) 방정식을 채택하였다. 계산된 파고는 측정된 파고와 잘 일치하고 있어 MAC 법이 유효함을 보여주고 있다. 한편, 비점성 불안정성 해석에 의해 유도된 Sub-breaking파 출현의 임계조건이 비대선수주위의 계산된 결과에 적용되었다. 이 유도된 임계조건이 Sub-breaking파의 출현을 잘 탐지하는 것을 확인하였다.

---

발 표 : 1991년도 대한조선학회 춘계연구발표회('91. 4. 13.)

Manuscript received : May 15, 1991, revised manuscript revised : August 29, 1991.

\* Member, Korea Research Institute of Ships and Ocean Engineering

## 1. Introduction

It is important to verify the flow field around a blunt bow in the field of ship hydrodynamics. But, the wave-breaking phenomena and nonlinearity on the free-surface around the blunt bow have not been come to knowledge.

The flow field around a blunt bow was simulated by Miyata et al.[1]. Finite difference method was adopted on the staggered rectangular grid system while the marker segments are moved by Lagrangian technique. The comparison with the measured results showed that the method was useful for the determination of better hull form with smaller wave resistance.

Grosenbaugh et al.[2] investigated the flow characteristics of the bow waves. There is a critical flow velocity at which the bow wave-breaking takes place. At the critical flow velocity, the bow wave develops a periodic oscillation. This oscillation appears to be due to the balance between the rates at which it is existing in quiescent condition.

Mori[3,4] suggested the sub-breaking waves as a free-surface turbulent flow which was transited from the laminar to turbulent flow. By the direct observation of the free-surface and the analysis of measured data, it was clarified that the sub-breaking waves was neither overturning nor spilling.

The term sub-breaking is used here for the steady breakers at an infant stage to distinguish from plunging or spilling-type breakers. When the oncoming flow velocity is increased, the steady breaker suddenly appears at a certain velocity; neither plunging nor spilling flows are observed then. It can be assumed a kind of free-surface turbulent flow with intensive fluctuations and it can not be categorized in the plunging or in the spilling breakers. The flow mechanism must be comparably different between them.

Sub-breaking waves by a submerged 2-dimensional hydrofoil were studied by Shin[5]. Experiments were carried out in detail to find out a turbulence model. Relating the turbulence terms with the averaged velocity, 0- and k- equation models

were introduced. Then by making use of these models, sub-breaking waves were simulated and compared with the measured results. The scheme with turbulence models simulated rather well the free-surface turbulent flow field with sub-breaking.

In the present paper, previous works are summarized concerning to the finite difference method applied for the explanation of the waves generated by a practical hull form and a series 60 models. Meanwhile, instability analysis of free-surface flow is applied to numerical results to detect the sub-breaking waves around a blunt bow in the critical flow velocity region. The qualitative accuracy of calculated results is examined and the quantitative availability of instability analysis is discussed.

## 2. Numerical Algorithm

### 2.1 Computational Procedure

The principal procedure and details of the TUMMAC-IV method are explained in previous references[1, 6, 7]. Therefore, very brief explanations are described here. The conservative formed Euler equations and continuity equation for inviscid and incompressible fluid are represented in finite-difference forms. These governing equations are solved as an initial-value and boundary-value problems including free-surface condition using time-marching procedure and iteration methods.

A Cartesian coordinate system is employed, in which the  $x$ -axis is the centerline on the design load waterplane of a ship. The ship advances in the negative  $x$ -direction. A grid system by staggered semi-variable rectangular meshes is used for the increase of computation accuracy and applicability. The Euler equations are represented by first order forward differencing in time and first-order centered differencing in space except for the convection terms. The differencing of the convection terms are described by a hybrid scheme that is the combination of second-order centered differencing and donor-cell method. Also, the continuity equation is represented by second-order centered differencing in space.

The momentum equations and continuity equation give the Poisson equation for the pressure distribution. The source term of the Poisson equation is determined from the velocity field at each time step. Therefore, the momentum equations and the Poisson equation are the principal equations to be solved in present computational procedure. The momentum equations are hyperbolic to be solved as an initial-value problem and the Poisson equation is elliptic to be solved as a boundary-value problem. That is, the former are solved by time-marching procedure and the latter is solved by iteration method at every time step.

The Poisson equation is iteratively solved by SOR(Successive Over Relaxation) method with the following equation.

$$P_{ij,k}^{m+1} = P_{ij,k}^m + \omega(P_{ij,k}^{cdl^{m+1}} - P_{ij,k}^m) \quad (1)$$

Where, the superscripts  $m$  and  $(m+1)$  denote iteration number and  $\omega$  is a relaxation factor.

$P_{ij,k}^{cdl^{m+1}}$  is temporary pressure at each iteration step. The iteration is continued until the second term of Eq.(1) converges within an allowable error.

The term in the parentheses in Eq.(1) is modified by eliminating  $P$  using the momentum equations. If the divergence  $D_{ij,k}$  is assumed in each staggered mesh, Eq.(1) is deformed as

$$P_{ij,k}^{m+1} = P_{ij,k}^m - \frac{\omega}{DT \cdot A} \cdot D_{ij,k} \quad (2)$$

The method by Eq.(2) is called the simultaneous iterative method which is equivalent to the SOR method. In this method velocity is successively updated through the iterated calculation of pressure field at a time step. This procedure is conveniently used to deal with the boundary condition for an arbitrary hull configuration.

Although this computational procedure is suitable to unsteady problems, it is applied to a steady problem of ship wave-making in this work by letting an unsteady solution approach to a steady state. The initial condition is a rested state, and

the velocities in computational domain are gradually accelerated for a desired incident velocity at the inflow boundary. After the steps of acceleration the computation is continued for an adequate time steps until a steady state is reached.

## 2.1 Boundary Conditions

The TUMMAC-IV method is aimed to simulate flow around a half body of a ship. Therefore, the computational domain is bounded by six boundaries including the centerplane, body and free-surface boundaries.

At inflow boundary the velocities are given as desired values i. e., in case of a Dirichlet problem. The computational domain is bounded by a center plane of a ship, because the flow of a ship is symmetry. Namely, on the centerplane the condition of symmetry must be taken into account. The bottom boundary is usually located so deep that the fluid motion is very small. Therefore, the hydrostatic pressure and the velocity condition of zero gradient are given at bottom boundary. At the sideward open boundary the velocities and pressures are set equal to the inner values so that their gradient in the direction normal to the boundary is set zero, i. e., in case of a Neumann problem. Also, at the downstream open boundary, their gradient along the local flow direction is set zero.

The hull surface is made of waterlines and framelines. The former is approximated by a succession of straight segments, and vertical variation within each cell is ignored for the latter. A free-slip body boundary condition is given in the body boundary cells(the cells included a body boundary segment). Namely, the velocity normal to a body surface is zero, and the tangential velocity does not have normal gradient, finally the divergence of a body boundary cell is zero. Under these conditions, the pressure of a body boundary cell is computed by velocity-pressure simultaneous iterative method.

On the free-surface, the Lagrangian movement of marker particles is used for the fulfilment of

the kinematic condition, and the irregular star technique of Chan and Street[4] is used for the dynamic condition. Some interpolation and extrapolation methods of velocities is made for the determination of the velocity components at the position of a marker particle, i. e., four-point and nine-point interpolations and zero gradient extrapolations are used.

### 3. Appearing Condition of Sub-Breaking Waves

Although the physical phenomenon corresponding to the calculated flow field shows sub-breaking waves, the calculation reaches the steady state without any trouble. The calculated result without any turbulence model or equivalent treatment about sub-breaking waves may be a fake. Thus, it is important to detect the appearance of sub-breaking from calculated results.

Mori introduce the appearing condition of sub-breaking waves by inviscid instability analysis, while reference[4] gives a full explanation.

As instability analysis for two-dimensional flows provides a critical condition for their appearance:

$$\frac{U}{M} \frac{\partial M}{\partial s} - \frac{\partial U}{\partial s} - \frac{1}{n_z} \frac{\partial n_z}{\partial s} > 0 \tag{3}$$

where,

$$M = (kU^2 - n_z g) n_z \tag{4}$$

$s$  is the stream line coordinate along the free-surface and  $h$  is its metric coefficient, while  $n$  is the normal to the free-surface;  $n_z$  the direction cosine of  $n$  to  $z$ .  $U$  is the velocity component of the basic flow in the  $s$ -direction,  $k$  the curvature of the free-surface and  $g$  the gravity acceleration. Limiting ourselves to a narrow proximity to the wave crest, we assume  $n_z \doteq 1$ ,  $\frac{\partial}{\partial s} \doteq \frac{\partial}{\partial x}$ ; then Eq. (3) can be reduced approximately into

$$\frac{U^2}{M} \frac{\partial}{\partial x} \left( \frac{M}{U} \right) > 0 \tag{5}$$

where

$$M = kU^2 - g \tag{6}$$

The negative gradient of  $M/U$  with respect to  $x$  means the flow can be unstable and sub-breaking can be appear (note here  $M$  is negative), while positive gradient means its stability.

Although the flow around the blunt bow is not two-dimensional, the three-dimensionality may not

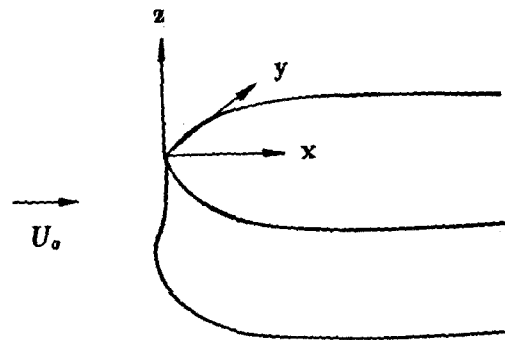


Fig. 1 Coordinate system

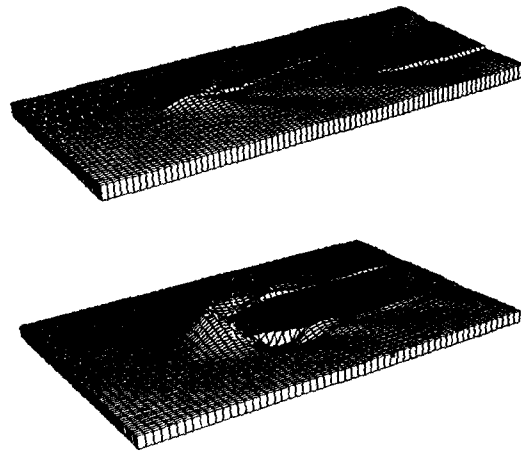


Fig. 2 Perspective views of computed waves (Series 60 models,  $Fn=0.2$ , from above:  $Cb=0.6, 0.8$ , wave height is three times magnified)

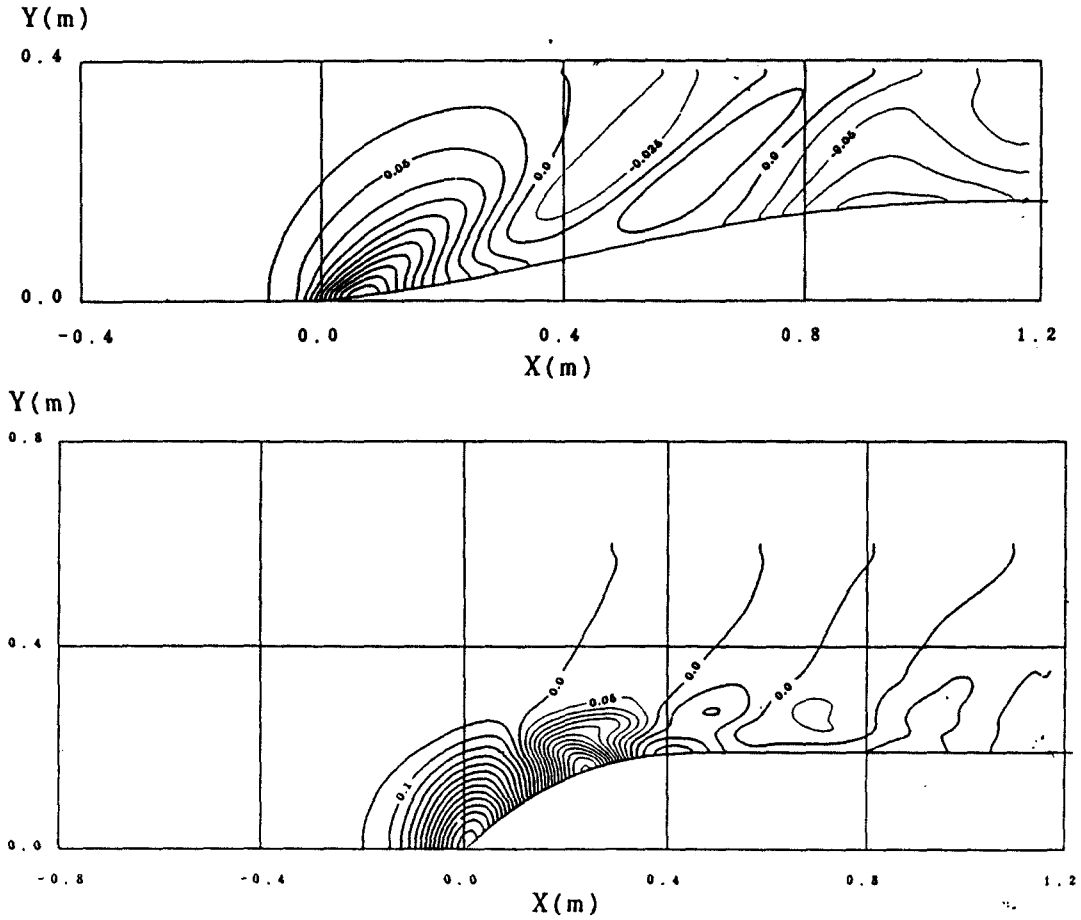


Fig. 3 Contour maps of computed waves(Series 60 models,  $F_n=0.2$ , from above :  $C_b=0.6, 0.8$ )

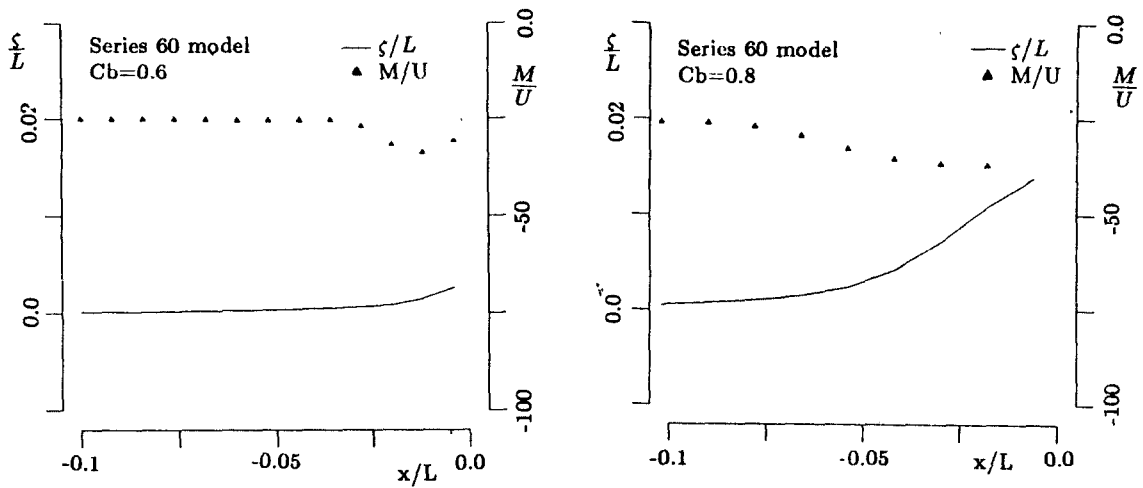


Fig. 4 Distribution of  $M/U$ (Series 60 models,  $F_n=0.2$ , from above :  $C_b=0.6, 0.8$ )

Table 1 Computational condition

	Series 60		Practical
	Cb=0.6	Cb=0.8	Hull Form
Domain of Computation(m)			
Length	1.60	1.80	4.80
Breadth	0.385	0.60	1.58
Depth	0.42	0.43	0.86
Cell Size(m)			
DX	0.02	0.03	0.07
DY	0.007	0.015	0.04
DZ(Min.)	0.005	0.01	0.019
Number of Used Cell	154,000	60,000	39,000
Time Increment(sec)	0.0040	0.0027	0.0064 0.0057
Time Steps for Acceleration	300	400	300
Total Time Step	750	1000	500 500
Froude Number $F_r$	0.2	0.2	0.15 0.17
Length of Ship Model(m)	2.5	2.5	7.1341

be so strong that we can expect Eq.(5) is applicable without any significant errors.

4. Discussions

Ship hulls used in this study are series 60 models and arbitrary chosen practical hull form. That is a crude oil tanker that values of block coefficient and length by breadth are 0.804 and 5.48, respectively.

Fig. 1 shows the coordinate system and computational conditions are shown at Table 1 in detail. The number of grid points are 154,000 for series 60 models of Cb=0.6, 60,000 for Cb=0.8 and 39,000 for practical hull form.

Perspective views of computed waves which is magnified three times are shown at Fig. 2. The difference of wave configuration affected by block coefficient is noticeable.

Fig. 3 shows contour maps of computed waves. Wave height around bow by series 60 model of Cb= 0.8 is higher than that of Cb=0.6.

The appearing condition of sub-breaking waves

is applied to calculated results which is shown at Fig. 4. The gradient of plotted M/U shows insignificant negative gradient with respect to x axis. It means the weak sub-breaking waves can be

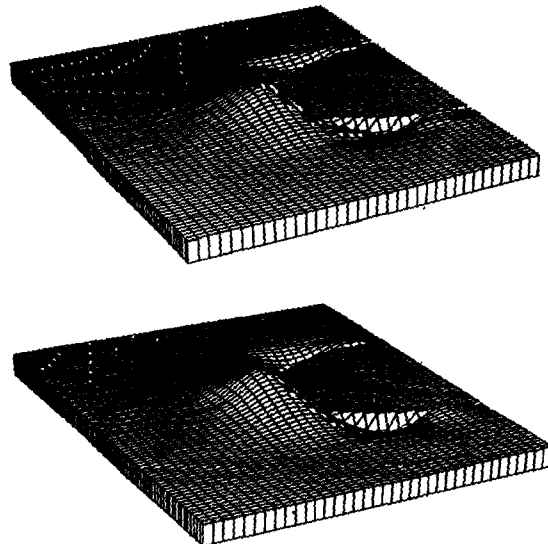


Fig. 5 Perspective views of computed waves (Practical Hull, from above :  $F_n=0.15, 0.17$ , wave height is three times magnified)

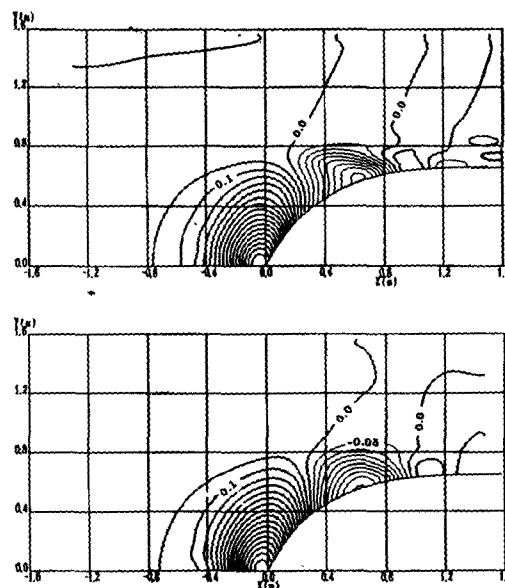


Fig. 6 Contour maps of computed waves (Practical Hull, from above :  $F_n=0.15, 0.17$ )

appear at this Froude number.

Fig. 5 shows the perspective view of calculated waves around a practical hull form while photographs of running ship model are shown at Fig. 7. The tendency of wave configuration seems good in agreement. Sub-breaking waves are physically shown around a bow but calculated results don't show this phenomena. Although calculated result shows smooth free-surface[Fig. 6] and the steady state is reached without any trouble, they are questionable. Therefore, it is necessary to adopt the numerical schemes for the sub-breaking waves or equivalent treatment.

Fig. 8 shows the  $M/U$  distribution applied to the calculated flow around a practical hull. The abrupt negative gradient with respect to  $x$  is shown which means the sub-breaking waves can be appear. As a result, this critical condition detects the appearance of sub-breaking waves.



Fig. 7 Photographs of running ship model  
(Practical Hull, from above :  $Fn=0.15, 0.17$ )

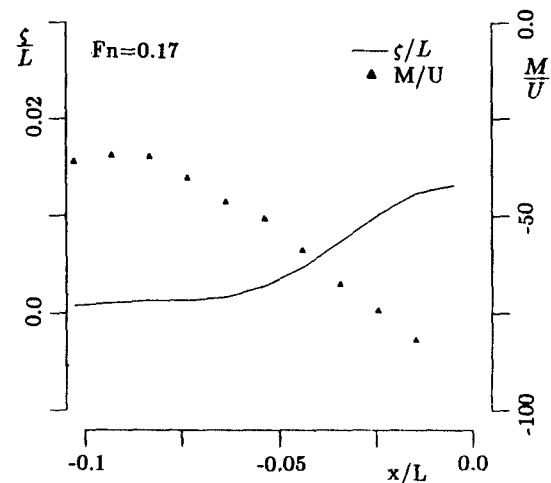
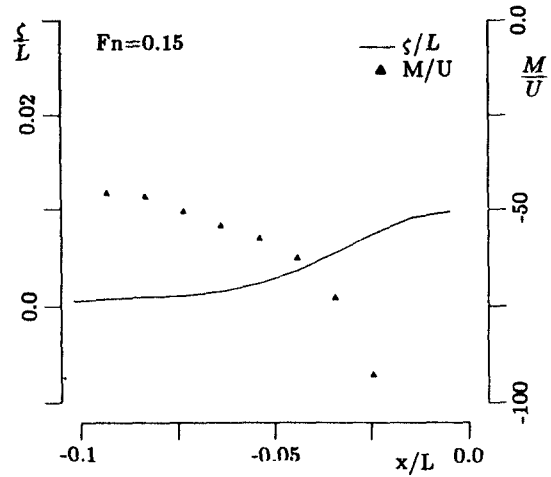


Fig. 8 Distribution of  $M/U$ (Practical Hull, from above :  $Fn=0.15, 0.17$ )

### 5. Conclusion

The flows around a blunt bow are numerically simulated by using MAC method and inviscid instability analysis is applied to the calculated results. Findings through the present study are summarized as follows:

1) The marker particles moved by Lagrangian technique simulate well the free-surface flow around a blunt bow with the appropriate body boundary condition.

2) By applying the appearing condition of the

sub-breaking waves derived from the instability analysis to the calculated results, it is confirmed that the condition detects the appearance of sub-breaking waves.

However, further efforts must be devoted for the simulation of sub-breaking waves, with the available turbulence model. It is important to clarify the mechanism of sub-breaking waves on the free-surface. The main frame of this work was done at University of Tokyo and Hiroshima University. All the computations were executed by IBM PC-386 with WEITEK coprocessor at Korea Research Institute of Ships and Ocean Engineering.

#### Reference

- [1] Nishimura, S., Miyata, H., and Kajitani, H., "Finite-Difference Simulation of Ship Waves by the TUMMAC-IV Method and Its Application of Hull-Form Design", *Journal of Society of Naval Architects of Japan*, Vol.157, pp.1-4, 1985.
- [2] Grosenbaugh, M.A. and Yeung, W., "Flow Structure Near the Bow of a Two-Dimensional Body", *Journal of Ship Research*, Vol.33, pp. 269-283, 1989.
- [3] Mori, K., "Critical Condition for Their Appearance of Steady Breakers on 2-Dimensional Wave Generated by Submerged Foil", *Nonlinear Water Waves*, Spinger-Verlag, pp.145-150, 1987.
- [4] Mori, K. and Shin, M.-S., "Sub-breaking Wave : Its Characteristics, Appearing Conditions and Numerical Simulation", *Proceedings of 17th Symposium on Naval Hydrodynamics*, 1988.
- [5] Shin, M.-S. and Mori, K., "On Turbulent Characteristics and Numerical Simulation of 2-Dimensional Sub-Breaking Waves", *Journal of the Society of Naval Architects of Japan*, Vol. 165, pp.1-8, 1989.
- [6] Lee, Y.-G., Miyata, H. and Kajitani, H., "Some Applications of the TUMMAC Method to 3D Water-wave Problems", *Journal of Society of Naval Architects of Korea*, Vol.25, No.4, pp. 13-27, 1988.
- [7] Cho, K.J., Lee, K.-H. and Lee, Y.-G., "A Numerical Simulation of Ship Waves by using Finite Difference Method", *Journal of Society of Naval Architects of Korea*, Vol.28, No.2, pp. 77-94, 1991.
- [8] Shin, M.-S., Lee, Y.-G. and Kang, K.-J., "Numerical Simulation of the Free-Surface Flow around a Floating Body", *Proceedings of 6th International Workshop on Water Waves and Floating Bodies*, 1991.
- [9] Chan, R.K.C. and Street, R.L., "A Computer Study of Finite-Amplitude Water Waves", *Journal of Computational Physics*, 6, pp.68-94, 1970.